THE OBSERVATION OF ELF-VLF RADIO NOISE WITH SOUNDING ROCKETS L-3-2, K-9M-6

Akira IWAI, Jinsuke OUTSU and Yoshihito TANAKA

Abstract

A project is now being carried on of observing radio noises in the ionosphere or the exosphere with the sounding rocket. Up to present, the data from L-2-2, L-3-2, and K-9M-6 were available, though the other two observations were missed due to the damages of the rocket or the telemeter system.

In order to measure the value of dispersion of whistlers and the frequency band of hisses two systems were used. The one is a point-frequency system using a whip antenna and several narrow band receivers and the other is a wide-band system using a loop antenna and a wide-band reciver.

The whistlers were observed, through both systems and the variation of the dispersion against the altitude has been estimated. On the one hand, a series of strong and periodically varying noises have been observed.

Because of their unusual intensity and sharp directivity, it is suggested that the strong noises observed may be caused by the electrostatic ion waves in the plasma.

1. Introduction

As described in the previous paper[1], the observation of the phenomena of electromagnetic waves, ranging ELF-VLF, in the ionosphere and the exosphere are being carried on by the sounding rocket, launched by the Institute of Space and Aeronautical Science, University of Tokyo.

After the previous paper, three rockets, L-3-2, L-3-2 and K-9M-6, were launched to observe the radio noise in the ELF-VLF bands. The data from L-3-2 and K-9M-6 were available, but the observation by L-3-3 was failed due to the damage of the rocket-borne receiving antenna.

In order to measure the value of dispersion of whistlers and the frequency band of hiss, a whip antenna and several narrow-band receivers were used in L-3-2 and L-3-3. On the other hand, a loop antenna and a wide band receiver were installed in K-9M-6. This paper describes the method of the observation and some discussions on the data obtained by L-3-2 and K-9M-6.

2. Observing Method

The observing method used in L-3-2 and L-3-3 was different from L-2-2. Being allocated several telemeter channels, 5 receivers for L-3-2, 4 receivers for L-3-3 were installed on the rockets. The observing frequencies and the band widths of these receivers are shown in Table 1.

Table 1. Observing Frequencies and the Band Width of the Receivers.

L—3—2		L—3—3	
Observing Freq.	Band Width	Observing Freq.	Band Width
500 c/s	100 c/s	500 c/s	100 c/s
1 kc/s	200 c/s	1 kc/s	200 c/s
1.5 kc/s	200 c/s	2 kc/s	200 c/s
3.5 kc/s	200 c/s	3.5 kc/s	200 c/s
8 kc/s	600 c/s		

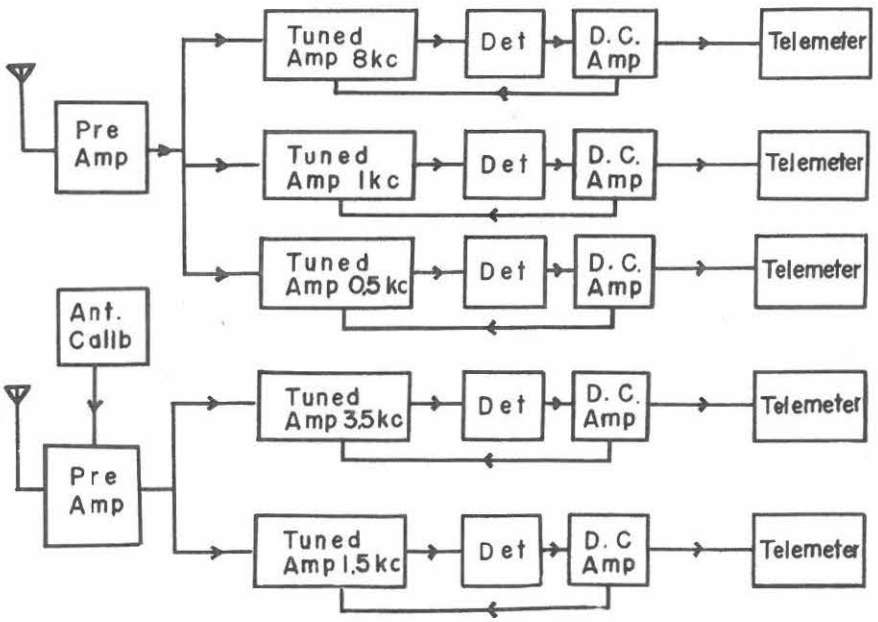

Fig. 1. Block diagram of observing apparatus (L-3-2)

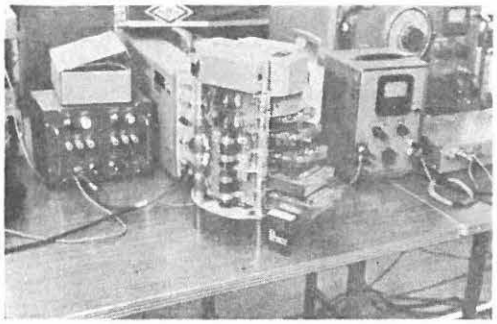

Photo. 1. Observing Apparatus installed in L-3-2

A set of whip antennas of 3 meters long were used for these two rockets. The output from the antenna was led to the preamplifier installed near the antenna, and after transformed to a low impedance, the output was introduced to each receiver. The signal to noise ratio of each receiver was 10 dB for the input signal of 10 micro-volts and the dynamic range was 60 dB. The time constant of the detector and the AGC circuit of each receiver were the same as for L-2-2. The output signal of each receiver was detected by a detector, transformed into DC and then supplied to the telemeter transmitter respectively. The block diagram of the circuit used in L-3-2 is shown in Fig. 1. And Photo. 1. shows the observing apparatus installed in L-3-2.

For K-9M-6, on the other hand, a loop antenna of 1.3 meters square and a wide-band receiver system were employed because of the unknown characteristics of the whip antenna in the plasma. The receiving frequency range was from 400 c/s to 10 kc/s. The sensitivity of the receiver was automatically controlled by its average output of the detector. The detector had the charging time constant of 0.2 sec., discharging time constant of 30m sec. and AGC time constant of 1.5 sec. The dynamic range of this receiver was about 40 dB. During flight, therefore, this wide band receiver was expected to operate at a moderate gain by this AGC system.

For the telemetering of this wide-band signal observed by this receiving system, a wide-band telemeter system, up to 10 kc/s, was also installed on the rocket. To know the operating gain of the receiver at every point of the trajectory, the AGC voltage was also telemetered to the ground. The block diagram of the circuit employed in K-9M-6 is shown in Fig. 2. Photo. 2. shows the observing apparatus installed in K-9M-6.

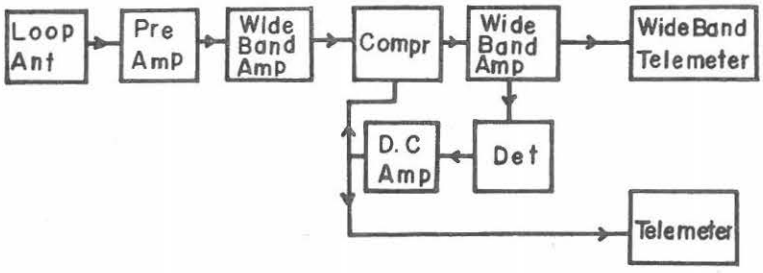

Fig. 2. Block diagram of observing apparatus (K-9M-6)

For comparison, simultaneous observation on the ground was made at Takakuma, about 40 km away from Kagoshima Space Center.

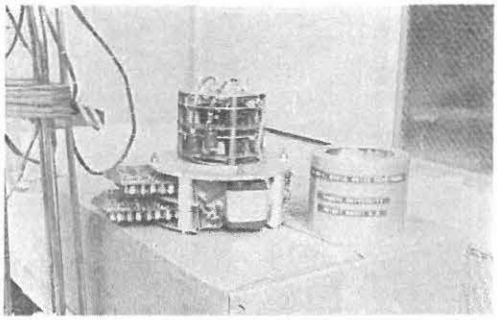

Photo. 2. Observing Apparatus installed in K-9M-6

3. Observational Results and Disccussions

3.1. L-3-2 Rocket Experiment

3.1.1 General

The L-3-2 rocket was launched from Kagoshima Space Center with azimuthal angle of 146° at 1401 JST on January 31st, 1965. This rocket was consisted of three stages, i. e., first booster, second booster and main rocket which were connected in series.

The receivers of radio noises were installed on the second booster in order to avoid interfering noises coming from an aspectometer of magnetic flux-gate type and ionospheric resonance probes which were installed on the main rocket.

The second booster reached the maximum altitude of 337 km at 300 seconds after the launching. Its trajectory is shown in Fig. 3. During the flight three types of signal were recorded at the launchang site. Two of them indicate pulsive nature and the remainning one is of epriodic nature. One of the pulsive types is caused by

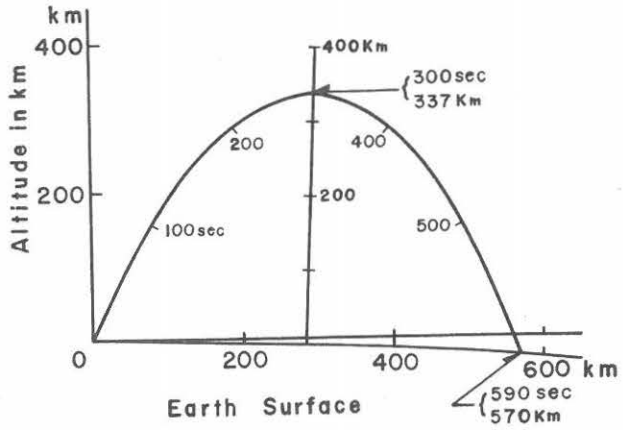

Fig. 3. Trajectory of the second booster of L-3-2 rocket

whistlers as will be described below, while the other pulsive type of signal has been thought to be produced in the telemeter system during the time when field intensity of transmitted signal from the flying rocket is so weak that the synchronism of telemeter system is lost. We shall call this noise 'telemeter noise'. The telemeter noise occurrs simultaneously on all frequency channels, while signals of whistlers occur with regular time delays on each frequency channel, so the telemeter noise can be easily distinguished from whistlers.

3.1.2 Whistlers

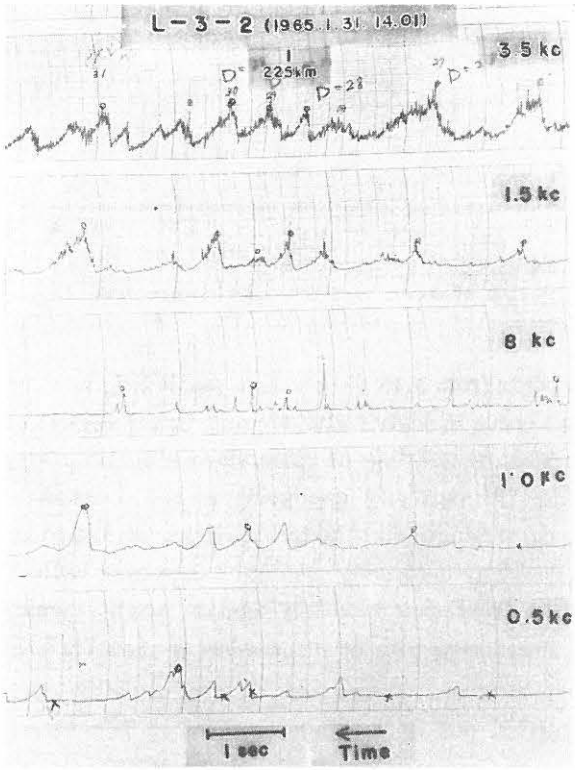

Fig. 4. Whistler signals received at five point frequencies
Relative time delays due to whistler dispersions can be seen.

Some examples of pulsive noise are shown in Fig. 4., which were receivd in the height range of 220km-230km on the ascending flight. On these records, systematic time delays can be seen for corresponding pulses on each frequency channel, although they do not always appear on all channels. The difference in shapes recorded on each channel will be due to dispersion characterisitics of whistlers as well as difference of circuit characteristics of each frequency channel.

From a careful measurement of the time delays it is found that these pulsive noises are caused by whistlers, because the delay times agree well with those of whistlers whose dispersions are 25-31 $\sqrt{\text{sec.}}$ By fitting method of time delay patterns, 109 whistlers have been detected along the trajectory from 110 km high on the ascent to 107 km high on the descent, and for 88 of them, dispersions have been decided. The telemeter noise and periodic noise increased on the descending flight, so that only a small number of whistlers were detected on the descending branch.

In Fig. 5. the dispersion distribution against the height is plotted, where closed circles are for the ascent and open circles are for the descent. The maximum value of dispersion is 31 $\sqrt{\text{sec}}$ and the minimum value is 25 $\sqrt{\text{sec.}}$ It can be seen from this

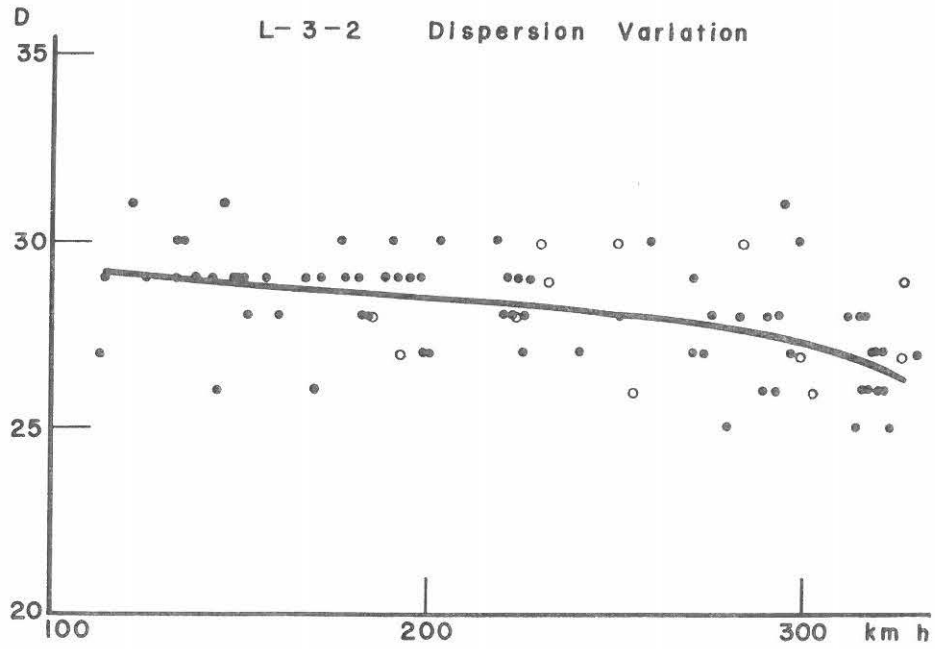

Fig. 5. Dispersion variation of L-3-2 whistlers against altitude
The closed circles show the case of ascent and the open circles show the case of descent.

plot that the scattering in dispersion amounts from 3 to 5 $\sqrt{\text{sec}}$ in a small height range and that smaller dispersions do not always occur in higher altitude and larger dispersion do not always occur in lower altitude. This scattering of dispersions may be partly due to varieties of whistler path passing through any one point in the ionosphere and partly due to errors in dispersion determination. Though variation of dispersion with heigh is not clear owing to the scattering, a running average taken over each 20 km at 10 km intervals, reveals a slightly decreasing tendency against height, which is expressed by a curve in Fig. 5. The decreasing rate of dispression is about $1\sqrt{\text{sec}}$/140 km below 250 km and $1\sqrt{\text{sec}}$/44 km between 250 km and 337 km.

A simultaneous observation was carried out on a ground station at Takakuma, about 40 km away from Kagoshima Space Center. During the flight of the rocket, 32 whistlers were observed at the ground station, but their intensity was generally weak, so the value of dispersion has been decided only for ten whistlers and the determination error will not be less than $5/2\sqrt{\text{sec}}$. Occurrence number and dispersion value during each one minute are shown in Table 2 together with those of rocket whistlers. The dispersion of ground whistlers varied from $25\sqrt{\text{sec}}$ to $35\sqrt{\text{sec}}$ and the average value was $30\sqrt{\text{sec}}$. This result shows that the dispersion of ground whistlers are comparable with those of rocket whistlers, thus it is likely that the ground whistlers came down through the base of the ionosphere near above the ground station.

Table 2. Results of simultaneous observation on L—3—2 rocket and Takakuma.

Time	Altitude	Rocket			Takakuma	
31 Jan. 1965		No.	Total *	Dispersion	No.	Dispersion
h m 14 02	km 0—190	35	31	26, 27, 28, 29, 30, 31	5	30
3	190—270	22	19	27, 28, 29, 30	6	30
4	270—320	23	18	25, 26, 27, 28, 29, 30, 31	3	25—27.5
5	320—337	10	8	25, 26, 27	5	27.5—30, 30
6	337—322	4	2	27, 29	5	
7	322—278	4	3	26, 27, 30	4	30
8	278—200	10	7	26, 27, 28, 29, 30	4	27.5—30, 30, 35
9	200— 0	1	0		0	

* Number of whistlers whose dispersion has been measured.

From the fact that 109 whistlers were observed on the rocket while only 32 whistlers were detected at the ground station, a screening effect of the ionosphere on the propagation of VLF radio waves is clear. This screening effect may be caused by the ionospheric absorption and partial and total reflections in the lower ionosphere.

In Fig. 6 average intensities of rocket whistlers during ascending flight are plotted against altitude, scaled with dB, 0 dB being 1 μv/m. This result shows that the intensity of 1.0 kc/s is strongest and that of 0.5 and 8.0 kc.s is very weak compared with 1.0 and 3.5 kc/s. Whistlers observed at Takakuma, on the other hand, have the most intense component at around 3.5 kc/s while at frequencies of 8.0, 1.0 and 0.5 kc/s no trace can be seen on sound spectrographs, and only at 1.5 kc/s a faint trace is seen in a few occasions. Thus we get a result that in the ionosphere the intensity of whistlers is stronger at 1.0 kc/s, than at 3.5 kc/s, while on the ground this is reversed. However, as the ionospheric absorption becomes greater as frequency increases, this result will be due to the noise level at the ground station which is higher at 1.0 kc/s than at 3.5 kc/s.

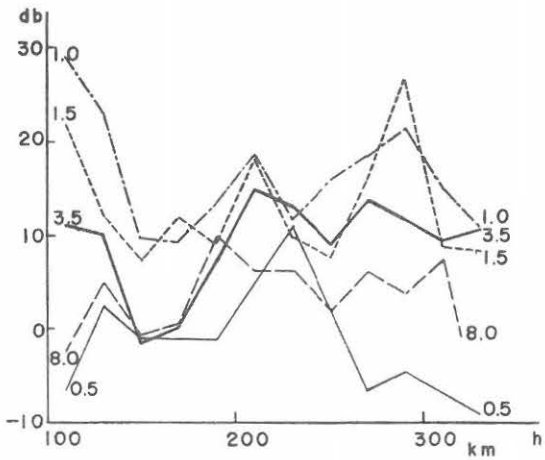

Fig. 6. Average intensities of L-3-2 whistlers during ascending flight

In Fig. 7 frequency distribution of

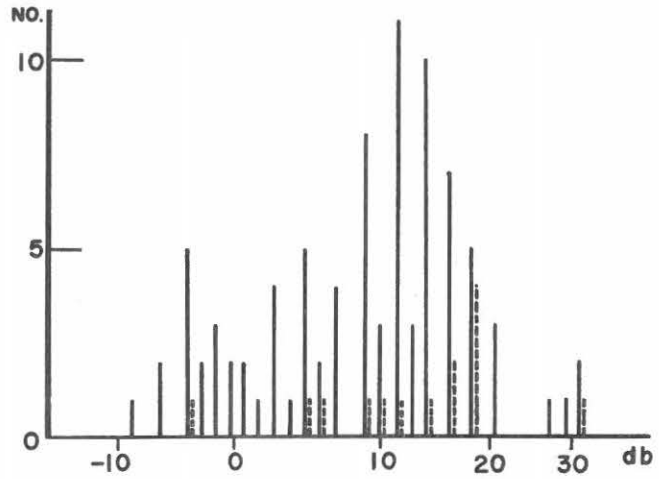

Fig. 7. Frequency distribution of intensity of L-3-2 whistlers measured at 3.5 Kc/s

intensity measured at 3.5 kc/s is shown. The dotted lines in this figure correspond to the whistlers observed simultaneously in the rocket and on the ground within one second. In general the measured intensity of rocket whistlers was weak. This phenomenon may be partly explained by the fact that, in most cases, the antennas are not oriented in a favorable direction to pick up the whistlers effectively owing to the spin and precession motions of the rocket (this will be disccussed later in some detail). At present it has not been known whether the whistlers observed simultaneously in the rocket and the ground within one second were really originated from the same lightning flashes or not. To make this clear, more precise time decision is needed, and to disccuss the screening effect of the ionosphere on whistler propagation, it is also necessary to know the true intensity of whistlers in the ionosphere and on the ground.

From this rocket experiment it has been made clear that in the ionosphere whistlers are detectable by the reception of whistler signals at several point frequencies. On the groud, however, this method has not been successfully carried out except for very intense whistlers, because at ground stations the level of interfering noises is comparable with the signal level of most of whistlers. In the ionosphere, on the other hand, it seems difficult to detect by this method long whistlers, echo-train whistlers, nose whistlers and ion-cyclotron whistlers, so that the wide-band observation is yet necessary for the detection of these types of whistlers as well as VLF emissions of isolate types.

3.1.3 Periodically varing radio noises

The records obtained in the flight range from about 150 km high on the ascent

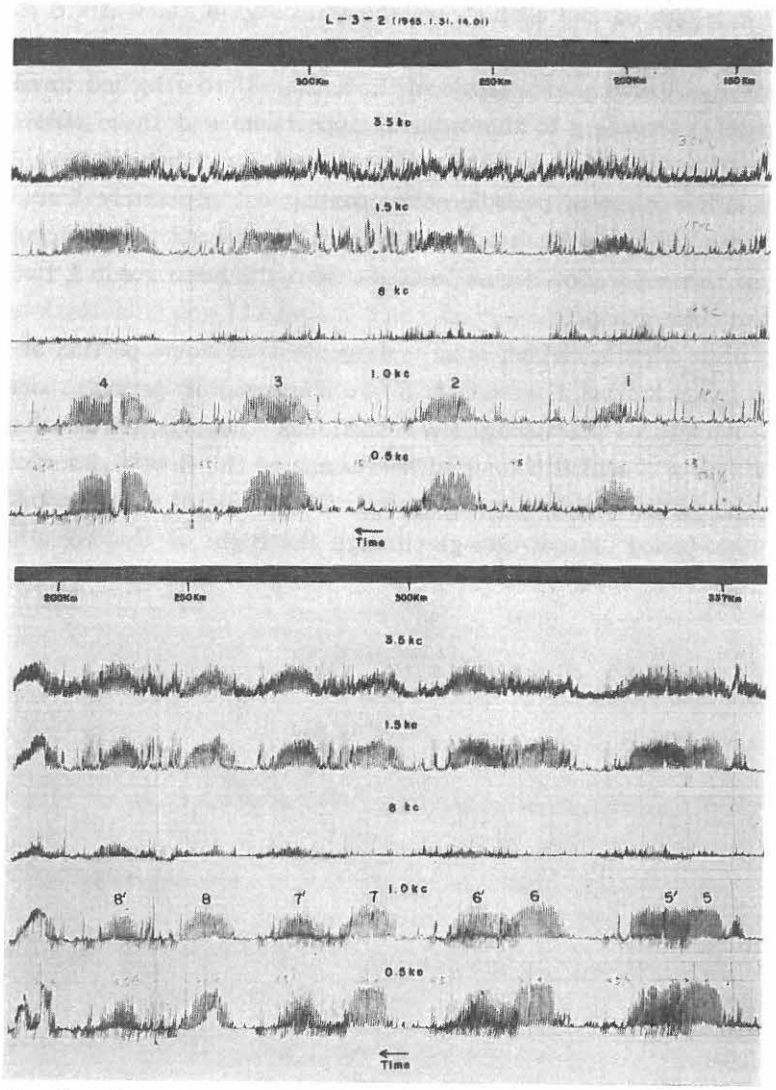

Fig. 8. Records obtained during the flight of the second booster of L-3-2 rocket

The upper shows the record during the ascent and the lower shows the record during the descent. 8 repetitions of intense periodically-varing noises can be seen as shown by labels 1, 2·····, 8 on the record of 1.0 kc/s channel. The labels of 5′,·····, 8′ are used for each of another group of periodic noises coming out separately from each group of 5,·····,8.

to about 200 km high on the descent are shown in Fig. 8, in which 8 repetitions of intense periodically-varing noises are seen on four frequency channels except 8.0 kc/s. On the record of 1.0 kc channel labels of 1, 2, ·····3 are attached to each group of the periodic noises according to the order of appearance and these noise groups will be called here-after 'the first series of noise groups'. The labels of 5'·····8' are used for each of another group of periodic noises coming out separately from each group of 5, ·····, 8 and these noise groups will be called "second series of noise groups". A tendency of this separation seems to begin from the noise group 3, but it becomes clear from the noise group 5.

As seen from Fig. 9, which is an enlargement of some portion of noise group 4, each noise group labeled 1, ·····, 8, 8' are composed of periodic noises of short period whose amplitudes are varing. We shall call these noises of short period as "short-period noises", which belong either to one of the first series of noise groups or to one of the second series of noise groups. The period of short-period noise is 4/3 seconds and this period did not change through the flight of the rocket, while the

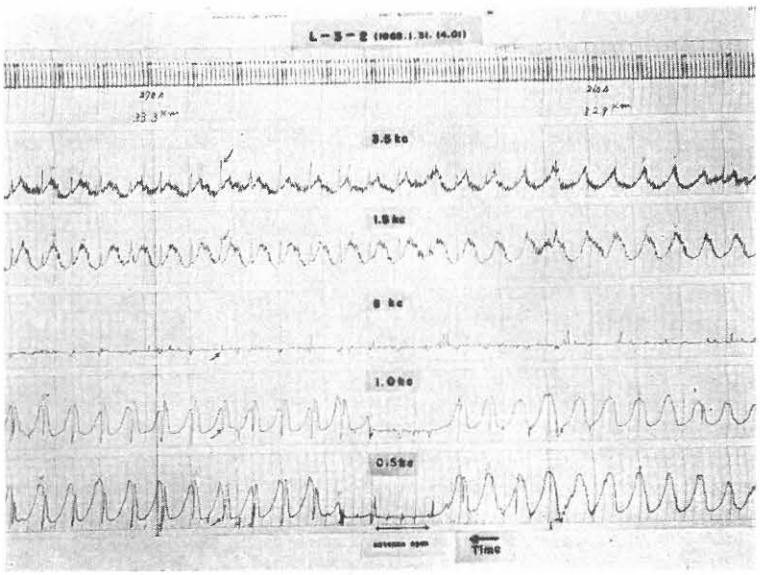

Fig. 9. An enlargement of the noise group 4
The arrow marks indicate natures of telemeter noise recorded on each frequency channel.
The steep fall of the noise amplitude to zero levels seen on the section of 1.0 and 0.5 kc/s channels, shown by "antenna open", was caused artifitially by opening the antenna circuit used for the reception of 1.0 and 0.5 kc/s. From this operation it is clear that the electric fields fetween antenna and rocket body have been picked up through the antenna.

repetition period of the first series of noise groups is about 45 seconds at the beginning of appearance and as the group number of the series increases it becomes slightly shorter. The repetion period of the second series of noise groups is about 47 seconds and it becomes slightly longer as the group number of the series increases.

In Fig. 10 peak intensities of each noise group of the first series are plotted against altitude. From these curves it can be seen that intensities of 1.0 and 0.5 kc/s are stronger than those of 1.5 and 3.5 kc/s and the maximum appear near the apex of the trajectory for 1.0 and 0.5 kc/s, but the intensities of 1.5 and 3.5 continue to increase without reaching any maximum. The maximum intensity of 1.0 kc/s exceeds 40 dB. The curves are not symmetric with respect to the apex and in general the intensity is stronger on the descent than on the ascent.

It can be seen from the records shown in Figs. 8 and 9 that the periodic noises sharply fall to zero level on the channels of 1.0 and 0.5 kc/s near the center of noise group 4, while such a falling does not occur on the channels of 3.5 and 1.5 kc/s. This falling of amplitude at 1.0 and 0.5 kc/s was caused artifitially by opening the antenna circuit used for the reception of 1.0 and 0.5 kc/s and connecting the input of the pre-amplifyer to the rocket body through a large capacitance with a timer equipped in the receiver. This operation was made automatically every minute. From this operation, it is clear that the electric fields between antenna and rocket body have been picked up through the antenna.

At present we can not conclusively decide whether these periodically appearing noises are originated in natural sources or not. But from the following facts they are very likely to be natural noise, (1) many whistlers were observed during the flight of the rocket and even during the periodic noises occurred they were also observed, (2) when the antenna was opened and the input of the pre-amplifyer was connected through a large capacitance to the rocket body the output of the receiver dropped to zero level, (3) between the noise groups zero levels were reached and (4) the periodicity was very regular. The fact of (1) means that the receiving apparatus

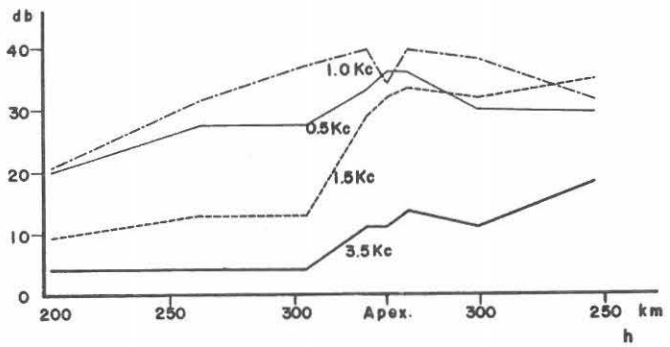

Fig. 10. Variation of maximum intensity of each noise groupe of the first series

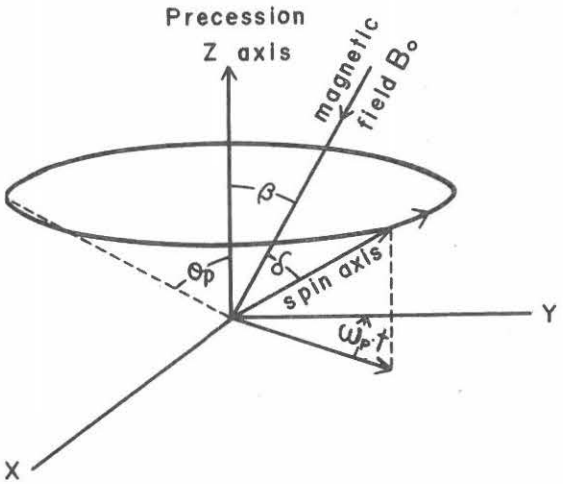

Fig. 11. Directions of precession axis, spin axis and local magnetic field β_o
β : angle between precession axis and β_o
θ_p : angle between precession axis and spin axis
δ : angle between spin axis and β_o
ω_p : precession angular frequency

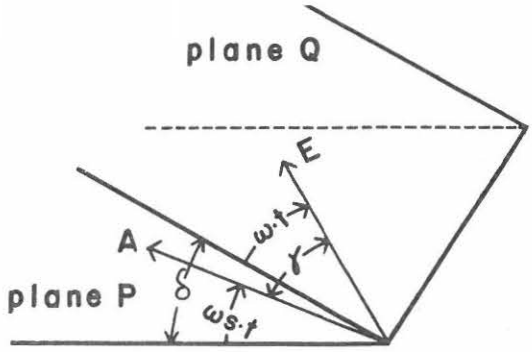

Fig. 12. Antenna A and electric field E of whistler mode wave
γ : angle between A and E
Q : a plane perpendicular to β_o in which E circularly rotates with ω.
P : a plane perpendicular to spin axis, in which A rotates with ω_s.
ω : wave angular frequency
ω_S : spin angular frequency

including antennas operated normally, the fact of (2) will show that electric fields between the antenna and rocket body were picked up through the antenna and the facts of (3) and (4) seem to support that the periodic noises are not artifitial ones arising from scientific apparatus in the rocket.

If we assume that the source of periodic noises is electric field of a wave propagating with constant polarisation and amplitude, the periodic amplitude variations will be produced through the variation of antenna direction relative to the electric field due to the spin and precession motions of rocket. Then the periodic amplitude variation of short-period noises will correspond to the spin motion and the periodicity of noise groups will correspond to the precession motion. Let us examin the relations between rocket motion and amplitude variation.

In Fig. 11 directions of precession axis, spin axis (rocket axis) and local magnetic field β_0 are schematically shown, where δ is the angle between spin axis and local magnetic field and it is given by

$$\cos\delta = \sin\beta \cdot \sin\theta_p \cdot \cos\omega_p t + \cos\beta \cdot \cos\theta_p \cdots\cdots\cdots\cdots (1)$$

where β is the angle between precession axis and β_0, θ_p is the angle between spin axis and precession axis and ω_p is precession angular frequency.

As the propagation mode of electromagnetic waves in the ionosphere is whistler mode only in the VLF range, we consider at first the amplitude variation of whistler mode wave by the rocket motion. In Fig. 12 planes Q and P are perpendicular to

the local magnetic field and spin axis respectively, so that the angle between planes Q and P is equal to δ. In the ionosphere the QL condition of whistler mode wave is still hold even when the wave normal direction relative to β_0 approches to right angle, so it can be safely assumed that the electric field E of whistler-mode wave is always vertical to β_0. Therefore, E lies in the plane Q rotating circularly with a

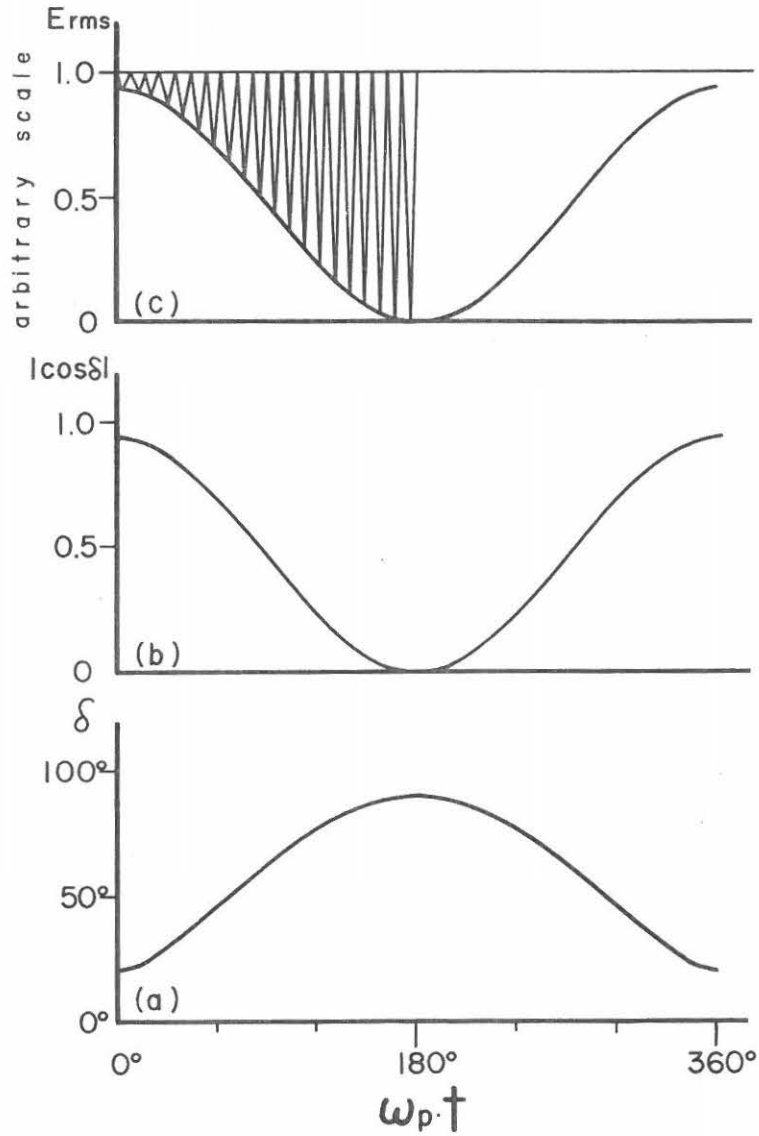

Fig. 13. Variation of rms electric field, E_{rms}, for a constant whistler mode wave during one precession period
(a) : Variation of the angle δ between spin axis and local magnetic field
(b) : Lower envelop of E_{rms}
(c) : Variation of E_{rms} due to spin motion

wave angular frequency ω. As the antenna is fixed vertically to the rocket axis, it rotates with spin angular frequency ω_s in the plane P. Thus, the angle γ between E and antenna A will be expressed, taking suitable time origin, as

$$\cos\gamma=\sin\omega t\cdot\sin\omega_s t+\cos\omega t\cdot\cos\omega_s t\cdot\cos\delta \quad\cdots\cdots(2)$$

As $\omega\gg\omega_s\gg\omega_p$, during the time when E rotates once, $\omega_s t$ and δ will stay almost constant. Consequently, the *rms* field intensity picked up by the antenna is given by

$$E_{rms}=\left\{\frac{\omega E_0^2}{2\pi}\int_0^{2\pi/\omega}\cos^2\delta\cdot dt\right\}^{\frac{1}{2}}$$

$$=\frac{E_0}{\sqrt{2}}(\sin^2\omega_s t+\cos^2\omega_s t\cdot\cos^2\delta)^{\frac{1}{2}} \quad\cdots\cdots(3)$$

where E_0 is the maximum amplitude of whistler mode wave.

During one rotation of the rocket by the spin motion $\omega_s t$ increases by 2π, but as $\omega_s\gg\omega_p$, δ stays nearly constant. Therefore, it can be seen from Eq. (3) that during one rotation of spin motion E_{rms} takes the minimum vale of $\frac{E_0}{\sqrt{2}}\left|\cos\delta\right|$ at $\omega_s t=0$, π and takes the maximum value of $\frac{E_0}{\sqrt{2}}$ at $\omega_s t=\frac{\pi}{2}$, $\frac{3\pi}{2}$, so that E_{rms} oscillates twice during one cycle of the spin motion. On the other hand δ varies according to precession motion as shown in Eq. (1).

Thus E_{rms} varies during one cycle of precession as shown in Fig. 13 (c), which is obtained under conditions $\theta_p=55°$, $\beta=35°$ so that $\delta_{max}=90°$. The E_{rms} calculated for whistler mode wave does not generally fall to zero level during each cycle of the spin motion and takes a constant maximum level of $\frac{E_0}{\sqrt{2}}$ independently of the precession motion. This variation of E_{rms} does not agree with the periodically-varing noises observed. Accordingly, the assumption of whistler mode wave is not suitable for the explanation of periodic noises.

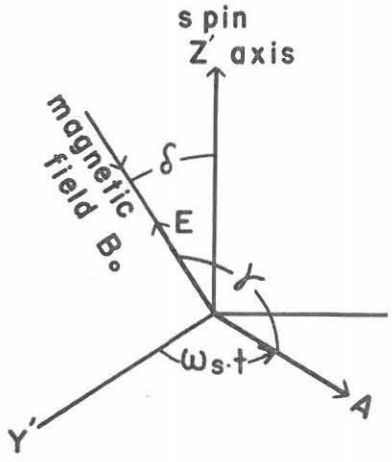

Fig. 14. Antenna A and electric field E of longitudinal electrostatic wave

Here, it should be remarked that E_{rms} produced by whistlers may take different values between $\frac{E_0}{\sqrt{2}}$ and $\frac{E_0}{2}\left|\cos\delta\right|$ according to the direction of the antenna, so that in most cases field intensity deduced from the input of the antenna may be weaker than the true *rms* field intensity. And also should be remarked that if we assume that the intensity of a whistler is ecqual at all frequencies, the intensity picked up by the antenna generally different directions when each frequency component of a whistler reaches the antenna, as they propagate with relative time delay defined by dispersion. Consequently, it must be noted that there are some uncertainties in any quantiative

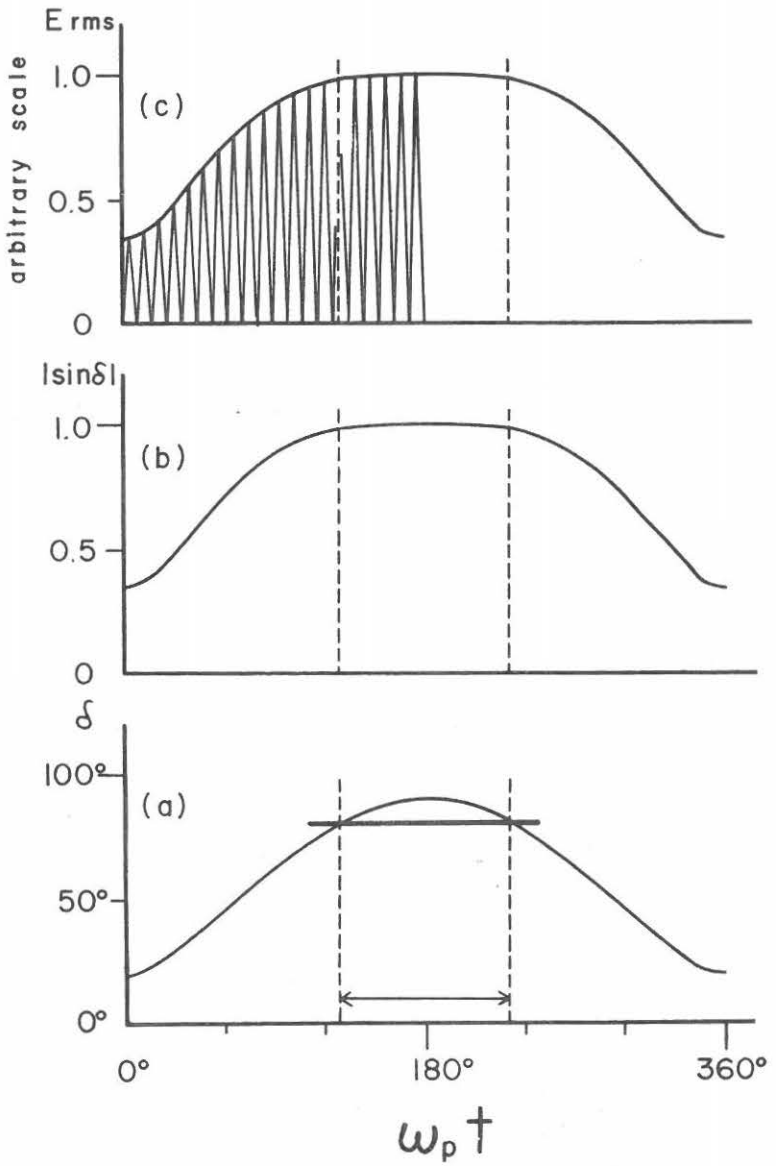

Fig. 15. Variation of rms electic field for a constant longitudinal electrostatic wave during one precession period : δmax=90°
(a) : Variation of the angle δ between spin axis and local magnetic field
(b) : Envelop of the maximum of each E_{rms}
(c) : Variation of E_{rms} due to spin motion
The section between dotted lines indicates a fractional part of one precession cycle when δ exceeds 80°

disccussions of intensity of each frequency of whistlers, unless E_{rms} picked up by the antenna is corrected with informations about antenna directions given by an aspectometer during the flight of the rocket.

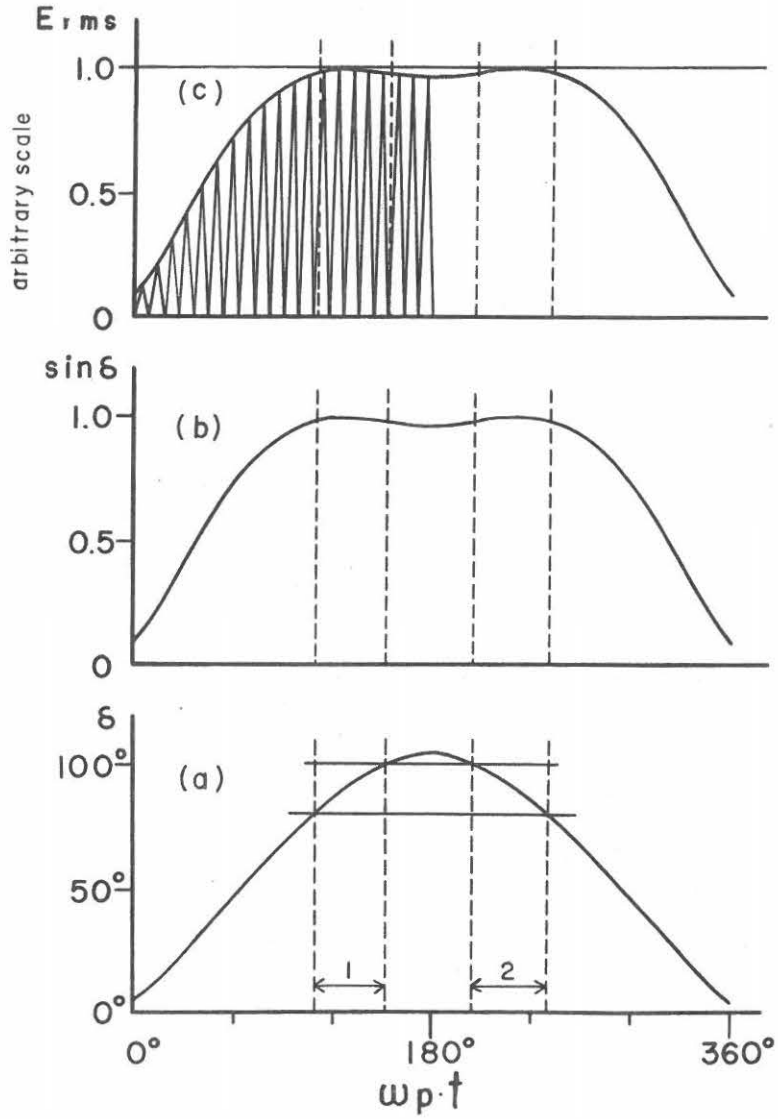

Fig. 16. Variation of rms electic field for longitudinal electrostatic wave during one precession period $\delta max=105°$
The envelope of E_{rms} has two peaks when δmax exceeds 90°
The sections 1 and 2 indicate fractional pats of precession cycle when δ lies between 80° and 100°

Now, let us consider an electrostatic wave linearly polarized along local magnetic field such as plasma waves suggested by F. L. Scarf et al[2]. In this case directions of electric field E, local magnetic field β and antenna A become as shown in Fig. 14 and the angle γ between E and A, is given by

$$\cos\gamma=\cos\omega_s t\cdot\sin\delta \cdots\cdots\cdots\cdots(4)$$

Then E_{rms} is expressed as

$$E_{rms}=\left\{\frac{\omega}{2\pi}\int_0^{2\pi/\omega}(E_0\cos\omega t\cdot\cos\delta)^2\,dt\right\}^{\frac{1}{2}}$$

$$=\frac{E_0}{\sqrt{2}}\left|\cos\omega_s t\cdot\sin\delta\right| \quad \cdots\cdots(5)$$

E_{rms} takes the maximum value of $\frac{E_0}{\sqrt{2}}\left|\sin\delta\right|$ at $\omega_s t=0,\ \pi$ and the minimum value equal to zero occurrs at $\omega_s t=\frac{\pi}{2},\ \frac{3\pi}{2}$ and it oscillates twice during one spin cycle. The calculated E_{rms} varies during one precession as shown in Fig. 15. (c), which is obtained under conditions $\theta_p=55°$, $\beta=35°$, so that $\delta_{max}=90°$. In this case the envelope of E_{rms} has a single peak. But when δ_{max} exceeds 90° two peaks occur as shown in Fig. 16 (c), which is obtained under conditions $\theta_p=55°$, $\beta=50°$, so that $\delta_{max}=105°$. And it will be easily understood that the separation between the two peaks of the envelope becomes longer as δ_{max} increases over 90°.

These variations of E_{rms} seem to agree in tendency with the variation of periodic noises observed. However, there are two problems here. The one is to explain the cause of no existence of periodic noises seen between noise groups and the other is to check whether δ_{max} can take a value which is large enough to explain the separation intervals between noise groups 5 and 5′, ……, 8 and 8′ or not.

The first problem will be solved if the pickup of electric field by the antenna does not obey the cosine law, instead the pickup decreases steeply outside a cone of narrow angle between electric field and antenna, that is if the antenna pickes up the electric field only when the direction of the antenna is nearly parallel to the local magnetic field. For instance, if we assume that this narrow angle is 10°, then the antenna will pick up the electric field during the time not over the one-ninth of each cycle of spin motion only when δ lies between 80° and 100°. Consequently,

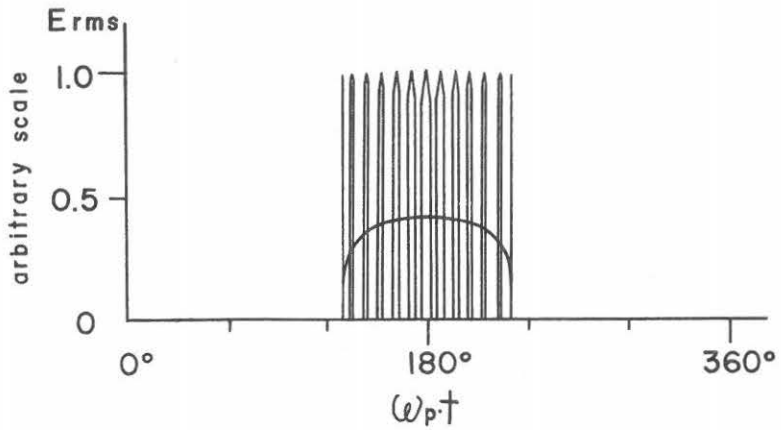

Fig. 17. Variation of E_{rms} when antenna pick up is confined within a narrow angle of cone 10° : δmax=90°

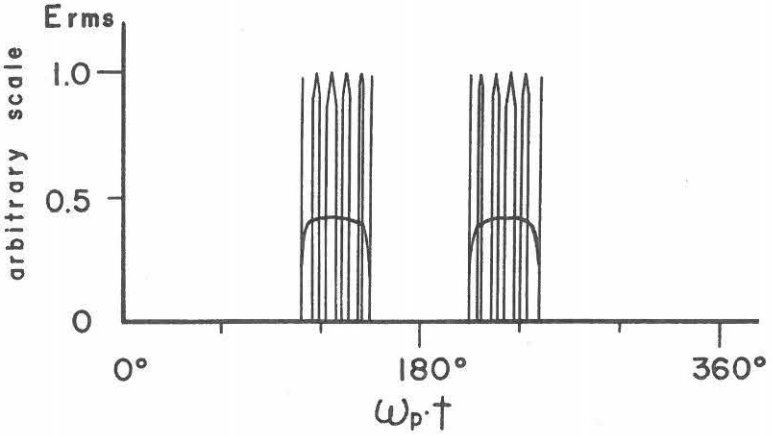

Fig. 18. Variation of E_{rms} when antenna pick up is confined within a narrow angle of cone 10° : δmax=105°

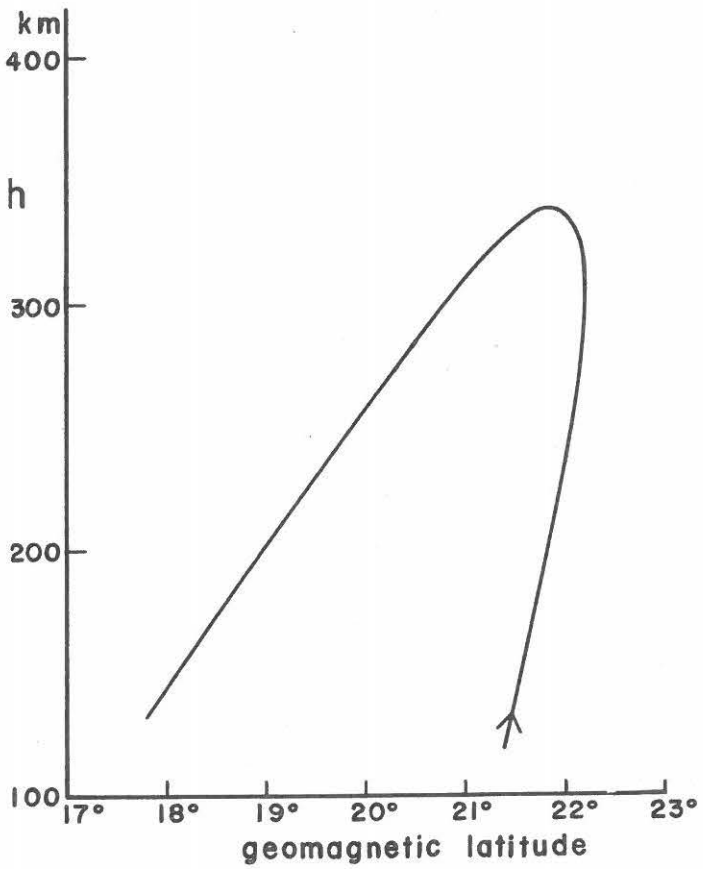

Fig. 19. Starting point in geomagnetic latitude of field line passing through each point along the trajectory of second booster of L-3-2 socket

under this assumption the E_{rms} will be observable only for some portion of one precession cycle but it will appear as a series of isolated pulses instead of a series of quasi sinusoidal pulses as seen on the records observed. This situation will be seen from curves of E_{rms} in Figs. 17 and 18 which correspond to the sections between dotted lines in Figs. 15 and 16 (a) and (b), drawn for $\delta=80°$ and $\delta=100°$ respectively. However, as the time constants of discharge of the VLF receivers are comparble with the period of periodic noises, the pulses picked up by the antenna under this assumption will be smoothed out and will form the periodic noises as observed. But owing to this smoothing-out their amplitude will be decreased as shown, for instance, by the curves in Figs. 17 and 18, which form envelopes of pulses of decreased amplitude. Under the assumption that the narrow angle is 10°, the two peaks of the noise group in Fig. 16 (c) become completely isolated as shown by the curves in Fig. 18, since the value of δ_{max} exceeds 100°.

Now, we consider the second problem. As seen above, there is a key to solve this problem in the magnitude of increment of δ_{max} and in the value of narrow angle of cone. It is easily known from Fig. 11 that the δ_{max} during one precession cycle occurrs when the spin axis lies in the plane determined by the precession axis and local magnetic field and that its value is equal to $\beta+\theta_p$. During the flight of the rocket, the angle θ_p between precession axis and spin axis is generally kept constant, consequently the increment of δ_{max} must be caused by the increment of β, e. i., through the change of direction of local magnetic field. In Fig. 19 the starting points in geomagnetic latitude of field line passing through each point along the trajectory is plotted against altitude. From this curve we can calculate the dip of field line along the trajectory. The variation in β obtained from this calculation amounts to only about 5.0° between altitudes of 200 km along the trajectory. In Fig. 20 values of δ_{max} is plotted against β for each value of θ_p. If we assume θ_p being 55° and the narrow angle being 10° as assumed above, β should take a value from 30° to 50° in order to give a value of δ_{max} from 85° to 105°, which is enough to separate another group completely from each single group of periodic variation.

This variation of β amounting to 20° is too large compared with the value of 5° calculated from the change of position of rocket along the trajectory. The variation of β needed entirely depends on the value of narrow angle of cone. so if we assume an extremely small value for the narrow angle of cone, this variation of β by 5° would be enouth to explain the complete separation of noise groups. If so, however, duration of isolated noise groups becomes too short to explain the observed phenomena. As we have had no informations about the aspect of the rocket, we have no means to know the values of θ_p and β. Accordingly, we can not estimate δ_{max} and the value of narrow-angle cone, and at present no clear reason have been known why longitudinal electrostatic waves have such an extreme directivity. Therefore we can not clearly explain the second problem now.

In order to confirm the disccussions above, following points should be made clear

by future observations of VLF waves with rockets equipped with aspectometers:

(1) the periodically varing noises actually exist or not,

(2) the period of short-period noises is half the spin period or not,

(3) the period of noise groups is equal to the precession period or not,

(4) the sharp directivity considered above exists or not,

(5) the separation of a noise group from each single noise group can be observed or not when δ_{max} increases over 90°.

If these periodically varing noises are really caused by longitudinal electrostatic waves, they will give us very inportant informations about the nature of irregularities in the ionosphere as well as the generation mechanism of longitudinal electrostatic waves.

3.2. K-9M-6 Experiment

The K-9M-6 rocket was launched from Kagoshima Space Center with azimuthal angle of 147° at 1902 JST on Feb. 6th, 1965. This rocket reched the maximum altitude of 332 km at 290 seconds after the launching. Its trajectory is similar to that of the second booster of L-3-2 rocket. In this case a loop antenna of 1.3 meter square was employed, which axis was parallel to the rocket axis. VLF signals ranging from 400 c/s to 10 kc/s were transmitted by a wide-band telemeter system and then recorded on magnetic tapes. During the flight 43 whistlers were observed. One example is shown in Fig. 20. The trace of this whistler on the sound spectrograph

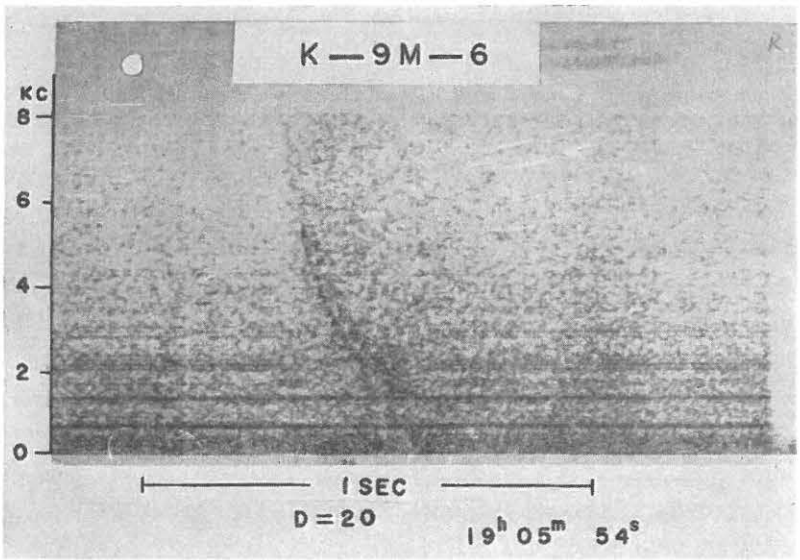

Fig. 20. One example of whistlers observed by a loop antennea

can be seen between 1.5 and 8.0 kc/s, but intensity of the rocket whistlers were generally weak and the measurement of dispersions was possible only for four whistlers. A simultaneous observation was made at Takakuma also. The results are shown in Table 3. The values of dispersions observed on the rocket and on the ground are nearly the same. Therefore, also in this case, whistlers seem to penetrate the lower ionosphere near above the ground station.

The dispersion value of 20 $\sqrt{\text{sec}}$ is small compared with the result by L-3-2 rocket. This may be due to the difference in electron density of the ionosphere between night and day.

It is interesting to note that any intense periodic noise corresponding to periodic noises observed by L-3-2 rocket was not detected aurally and spectrographycally. One reason of this will be that for electrostatic field a whip antenna is far more sensitive than a loop antenna.

Table 3. Results of simultaneous observation on K—9M—6 rocket and Takakuma.

Time	Rocket		Takakuma	
6 Feb. 1965	No.	Dispersion	No.	Dispersion
h m 19 02			1	
3	4			
4	7			
5	8	20	3	20
6	6		1	20
7	5		2	20
8	3			
9	6	17.5—20		

4. Conclusions

From the observations of VLF radio noises by L-3-2 rocket it has been confirmed that whistlers are detectable in the ionosphere by the reception of signals at several point frequencies. But by this narrow-hand-width method it seems difficult to detect long whistlers, echo-train whistlers, noise whistlers and ion-cyclotron whistlers, so that a wide-band telemetering is yet necessary for the reception of these types of whistlers as well as isolate types of VLF emission.

Simultaneous observations carried out on the rockets (L-3-2 and K-9M-6) and at the ground station at Takakuma give a general result that most of whistlers which

have normal dispersions at a ground stations may have penetrated the lower ionosphere near above the ground station.

In order to discuss quantitatively the intensity of whistles observed by rocket, it is necessary to know the direction of the antenna relative to the local magnetic field.

Intense noises of periodically varying type have been recorded on the frequency channels of 1.0, 0.5, 3.0 and 3.5 kc/s by L-3-2 rocket, though at 8.0 kc/s the intensity was very weak. It has been suggested that these periodically varying noises were caused by longitudinal electrostatic waves such as plasma waves. In this assumption, the periods of the short-period noises and the noise groups should correpond to spin and precession periods of the rocket respectively. However, in order to confirm this, further observations are necessary by a rocket equipped with an aspectometer.

5. Acknowledgements

We wish to express our thanks to Prof. A. Kimpara of Chubu Institute of Technology for his guidance and encouragement. Thanks are also due to Prof. H. Tanaka, the Director of our Institute, for valuable advice and kind help in the preparation of this paper and to Prof. K. Maeda, Prof. T. Obayashi of Kyoto Univ. for their help and advice and to Prof. A. Tamaki, Prof. S. Saito, Prof. T. Nomura, Prof. D. Mori and Prof. K. Hirao of the Univ. of Tokyo for loading the observing apparatus on the rocket. We are also indebted to Messrs. S. Urimoto, M. Oyama, of Meisei Electric Co. for constructing the observing apparatus. Finally, we appreciate very much the faithfull assistance of Messrs. T. Kato, T. Yamaguchi, M. Nakamura, M. Sato in the rocket observation.

References

(1) Iwai, A., Outsu, J. and Tanaka, Y. : Proc. Res. Inst. Atmospherics, Nagoya Univ., 12,11 (1965)

(2) Scarf, F.L., Crook, G. M. and Fredericks, R. W. : Jour. Geophys. Res., 70, 3045 (1965)